

**Details of the excellence in research work for which the Sun Pharma Science Scholar Award is claimed, including references and illustrations with following headings- Title, Introduction, Objectives, Materials and Methods, Results, Statistical Analysis, Discussion, Impact of the research in the advancement of knowledge or benefit to mankind, Literature reference. The candidate should duly sign on the details.**

**Title-** “Development of low-budget-biosensor for the detection of various deadly diseases towards commercialization”

### **Introduction**

Various deadly diseases (cancer, viruses) have become a global burden, with millions of people dying as a result of such life-threatening disorders. Despite significant advancements in the medical profession, no suitable medication or vaccinations are available to cure such disorders. Only a correct diagnosis can help you manage it. There are several diagnostic methods available, such as PCR, ELISA, and others, but these procedures have some drawbacks, including being highly expensive, requiring trained professionals, taking a long time, producing false/positive findings, being less sensitive, and being less specific. To address these constraints, an innovative developing method, namely, Biosensor, was used as a viable alternative for diagnosing such disorders. Biosensors have several benefits over traditional diagnostic procedures, including low cost, rapid response, on-site detection, no need for a specialist, and self-diagnosis. Extremely delicate and specific. The scientist used many sorts of biosensors, including electrochemical biosensors, colorimetric biosensors, optical biosensors, and piezoelectric biosensors. Electrochemical and colorimetric tests were the most common due to their simplicity of use and low cost. Electrodes are one of the main components in electrochemical biosensors, so scientist used the best of the best electrodes for the development of highly sensitive biosensors, but such electrodes were extremely expensive, which increased the cost of the

developed project, and these electrodes were made of plastic substrates, which are not good for our environment. So we have created self-fabricated electrodes on the normal paper with very less-cost , As a result, in this study, we employed several paper electrode configurations to build an electrochemical biosensor that detects dengue viral antigen with high sensitivity and low LOD, and also developed another effective and low budget biosensor i.e., colorimetric biosensor, In this work, we detected ovarian cancer by using a simple colour changing principle, so life-threatening diseases can be detected by using such simple colour magic testing, which helps millions of females, that they can easily detect their ovarian-cancer at an early stage so they can take proper treatment on time. As a result, we developed two low-cost biosensors that detect dengue virus and ovarian cancer with great sensitivity and selectivity.

**Objectives- In submitted project we have constructed two biosensor for the detection of dengue virus and ovarian-cancer.**

- a)-** Developed electrochemical paper based biosensor for the detection of dengue virus.
- b)-** Constructed self-fabricated paper electrode with the cost of 3 rupees.
- c)-** Developed colorimetric biosensor for the detection of ovarian cancer.
- d)-** Manufactured the nanomaterial by the help of chemical method and validate the results with SEM, TEM, XRD Uv-vis.

## **Materials and Methods (For dengue virus)**

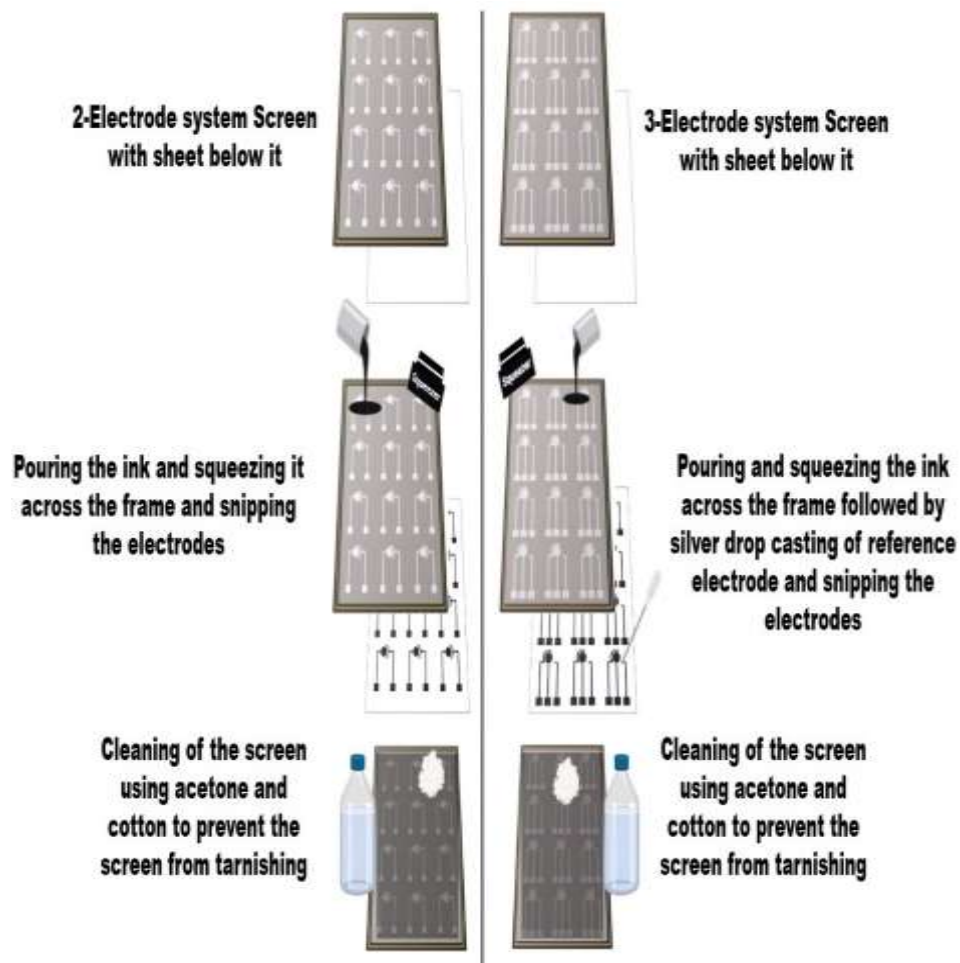
### **2.1. Chemicals, Reagents, and Apparatus**

Methylene blue was purchased from Sigma Aldrich, India, and all other chemicals were of AR grade. For the creation of paper electrode setups, A-4-size sheets in addition to silver conductive paste and black carbon conductive ink were acquired from Snab Graphix Pvt. Ltd. (Bangalore, India) NaCl, KCl,

Na<sub>2</sub>HPO<sub>4</sub>, and KH<sub>2</sub>PO<sub>4</sub> were acquired from LOBA to prepare PBS. The aptamer and antigen were prepared in PBS (pH 7.4, 100 M). The DENV-aptamer, a 34-base oligonucleotide, was purchased from MTOR life science Pvt. Ltd. and was complementary to the polyvalent DENV-antigen (Prospec-Tany TechnoGene Ltd. Israel). Aptamer sequence: GCACCGGGCAGGACGTCCGGGGTCCTCGGGGGGC [18]. Metrohm Dropsens (Stat-I 400s) were used for electrochemical experiments involving cyclic voltammetry (CV). Screen-printing frames were designed and purchased from a local project shop.

## **2.2. Fabrication and Features of Different Paper Electrode Setups**

In this study, two setups—the (a) two-electrode system and (a,b) three-electrode system—were constructed. Both of these systems were created using the screen-printing technique. In this technique, hand printing was performed using a silk screen with a lasercut patterned solid skin that was adhered to it and that had predetermined dimensions for a three-electrode arrangement. Carbon conductive ink (mainly composed of graphene, as it is a good conductor [19,20]) was squeezed onto cellulose sheets using a squeezer via the designated overhead screen's open areas. The silk screen was used as a stencil for the electrode preparation once the electrode's dimensions were set and framed on it. Three electrodes—a counter electrode (CE), a working electrode (WE), and a reference electrode (RE) drop cast with Ag/AgCl—made up the printed electrodes. As a result of this, the a three-electrode system was created, whereas the production of a two-electrode system involved all the same stages except for the fabrication of the reference electrode (Scheme 1 & Table 1).



**Scheme 1.** A comparative schematic representation of fabrication of two- and three-electrode systems.

**Table 1.** Comparative features of different paper electrode setups.

S.No Involvements		Two-Electrode System (a)	Three-Electrode System (b)
1.	<b>Total electrodes</b>	Two electrodes	Three electrodes
2.	<b>Name of electrodes</b>	of-Working electrode (WE)	-Working electrode (WE) -Counter electrode (CE) -Reference electrode (RE)

		-Counter electrode (CE)	
<b>3. Ink/paste</b>	Black carbon conductive ink	-Black carbon conductive -Silver paste casting for reference electrode	
<b>4. Substrate</b>	Paper (A-4-size sheets)	Paper (A-4-size sheets)	
<b>5. Fabrication method</b>	Screen-printing method	Screen-printing method	
<b>6. Incubation time</b>	Overnight	Overnight	
	<b>Electrochemical</b>		
<b>7. measurement for dengue detection</b>	Cyclic voltammetry technique	Cyclic voltammetry technique	
<b>8. Current range</b>	Low	Very high	
	<b>Expected price</b>		
<b>9. per electrode (INR)</b>	2 rupees (approx.)	5 rupees (approx.)	
<b>10. Preparation time</b>	3 min	5 min	
<b>11. Usability</b>	Prepare, use, and throw	Prepare, use, and throw	

### 3. Results

*3.1. Comparative Study of Current Amplification Based on Three- and Two-Electrode Setup, and Summarizing Their Differences in the Currents-*

### 3.1.1. Current Comparison of Different Stages of Aptasensor

For comparative study, first, we compared the currents of different stages of developing a dengue aptasensor. The four stages are: nanoparticles, aptamer, dengue antigen, and bare, which display different current responses based on two- and three-electrode systems. All these current range comparisons were confirmed by cyclic voltammetry (CV). Figure 1a,b show the differential current response at different stages of the electrode. In CV, bare electrodes displayed a lower peak current response, which is a consequence of slower electron transfer kinetics (Table 2). Due to the fast electron transfer kinetics offered by the silver/zinc nanocomposite, there was a large improvement in current responsiveness following its deposition onto the working surface. The non-conductive nature of the aptamer after immobilization onto the working surface significantly reduced the current. The well-known MB principle led to a further reduction in the current response after the introduction of an antigen. Intercalation of MB between bases drastically reduced the current response. This principle of stages is the same in both electrode setups.

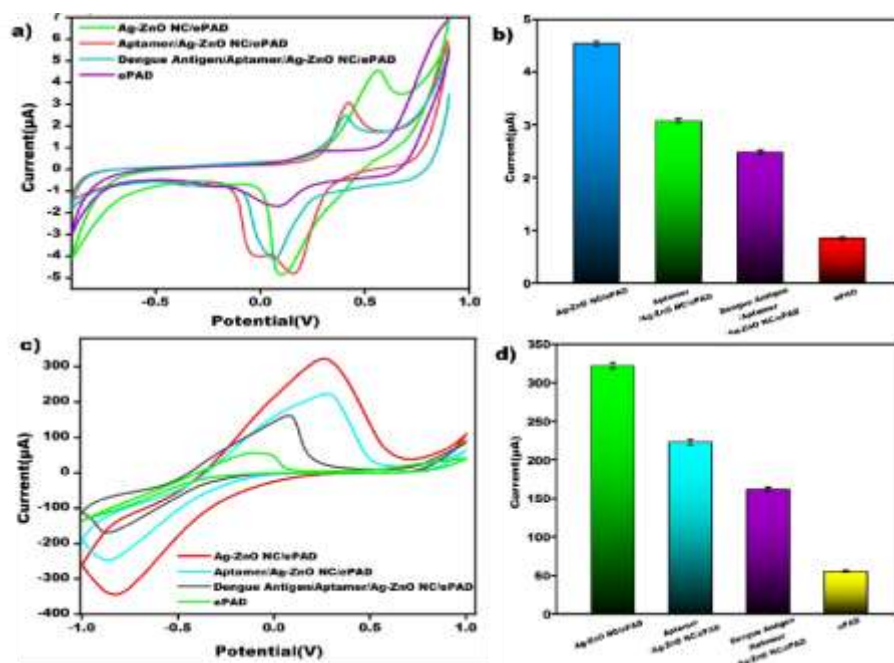


**Figure 1.** (a) CV of different stages of aptasensor showing different current ranges based on the two-electrode system. (b) Bar graph represents the different current ranges based on the two-electrode system. (c) CV of different stages of aptasensor showing different current ranges based on three-electrode system. (d) Bar graph represents the different current ranges based on the three-electrode system.

**Table 2.** Summarized the comparison of the different current ranges of the aptasensor stages based on different paper electrode setups.

S.No	Different Stages	Current (Two-Electrode Setup)	(Three-Electrode Setup)
1.	Nanocomposites	4.54 μA	322.21 μA
2.	Aptamer	3.07 μA	223.04 μA
3.	Antigen	2.48 μA	161.44 μA

<b>4. Bare</b>	0.85 $\mu\text{A}$	55.53 $\mu\text{A}$
----------------	--------------------	---------------------

---

### 3.1.2. Current Comparison of Different Concentrations of Dengue Antigen

The currents of different concentrations of the developed dengue aptasensor were compared. It involved four different concentrations of dengue antigen, i.e., 0.1, 1, 1.0, and 100  $\mu\text{g/mL}$ , which showed different current ranges based on two- and three-electrode systems. This current comparison of the developed aptasensor was validated by cyclic voltammetry (CV) (Table 3). A variety of concentrations, including 0.1, 1, 10, and 100  $\mu\text{g/mL}$ , were used in Figure 2a,b to facilitate aptamer hybridization. The findings showed that the antigen exhibits aptamer hybridization and that variable current responses were seen at various concentrations, confirming the constructed sensor's quantitative functionality. The outcomes are consistent with previously reported sensors. Since more insulating layers of the biological recognition element slow down the electron transfer, the current response decreased when antigen concentrations were increased. This principle of comparing the currents of different concentrations was the same in both electrode setups.



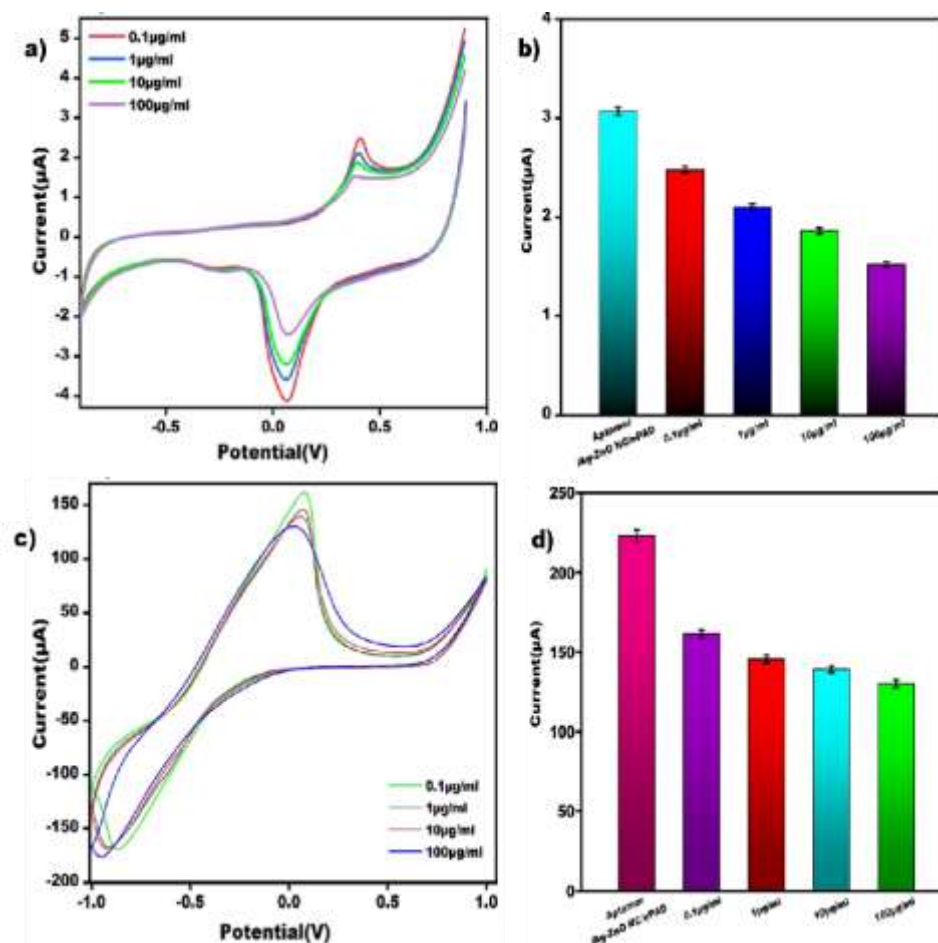


**Figure 2.** (a) CV of different concentrations of dengue antigen showing different current ranges based on the two-electrode system. (b) Bar graph of different concentrations based on the two-electrode system. (c) CV of different concentrations of dengue antigen showing different current ranges based on the three-electrode system. (d) Bar graph of different concentrations based on the three-electrode system.

**Table 3.** Summarized the comparison of the different current ranges of the different concentrations of dengue antigen based on different paper electrode setups.

S.No	Dengue Antigen Concentrations	Current (Two-Electrode Setup)	Current (Three-Electrode Setup)
1.	0.1 $\mu\text{g/mL}$	2.48 $\mu\text{A}$	161.44 $\mu\text{A}$
2.	1 $\mu\text{g/mL}$	2.10 $\mu\text{A}$	145.57 $\mu\text{A}$
3.	10 $\mu\text{g/mL}$	1.86 $\mu\text{A}$	139.20 $\mu\text{A}$
4.	100 $\mu\text{g/mL}$	1.52 $\mu\text{A}$	130.19 $\mu\text{A}$

Based on the above results, it is very clear why the three-electrode system is best compared to the two-electrode system in terms of high electron transfer, high current amplification, and its unique electrochemical principles as well.

### *3.2. Justification for Using Three-Electrode System over Two-Electrode System*

In the construction of a two-electrode system, only the counter and working electrodes are used. To begin the dengue virus detection mechanism, we first established the sensor by depositing nanoparticles on the circular region of the working electrode, then immobilized aptamer on the nanoparticles, and finally deposited dengue antigen followed by methylene blue (MB), which acts as an intercalating agent. Both electrodes were immersed in MB solution, and the current response was measured and confirmed using popular electrochemical parameter i.e., CV (Cyclic voltammetry). The response was measured upon the imposition of  $\Delta E$  potential between the two electrodes [21]. The sensing protocol was the same in both electrode systems except that the reference electrodes

were also dipped in MB along with counter and working electrodes, which significantly helps in enhancing the current range of the three-electrode-based biosensor [22] (Figure 3).

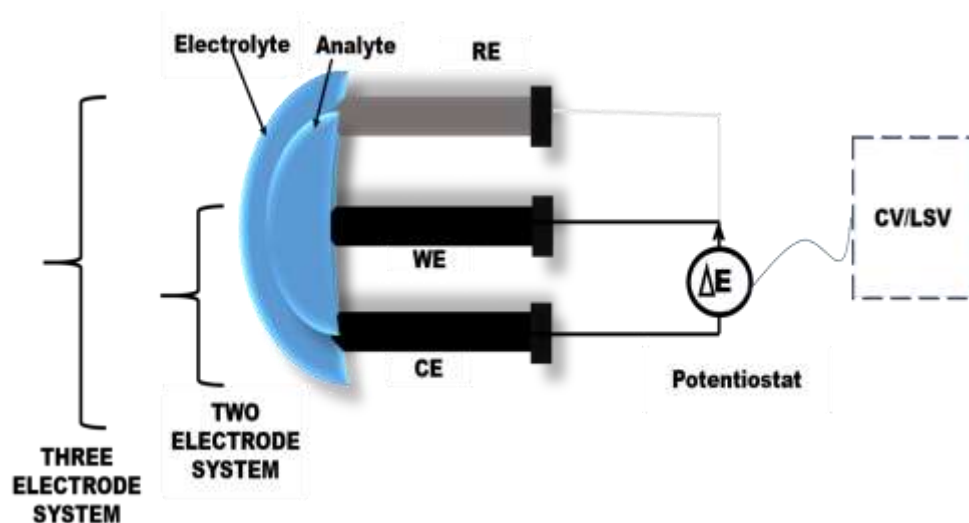


**Figure 3.** Working principle of two-electrode and three-electrode electrochemical setups.

**The two-electrode system** is made up of a working electrode, where the chemistry of interest occurs, and a counter electrode, which serves as the other half of the cell. The working and counter electrode potentials are measured, and the resulting current is measured in the working or counter electrode lead. In the two-electrode setup, the counter electrode serves two purposes. It completes the circuit, enabling charge to flow through the cell, and it also maintains a constant inter-facial potential irrespective of current. It is extremely difficult to maintain a constant counter electrode potential in a two-electrode system when current flows. **The three-electrode system**, on the other hand, addresses many of

the shortcomings of the two-electrode configuration. A working electrode, a counter electrode, and a reference electrode comprise the three-electrode system. The role of the reference electrode is to serve as a reference in measuring and attempting to control the working electrode potential while no current is passed through it. At low current density, the reference electrode has a constant electrochemical potential. Furthermore, because the reference electrode passes negligible current, the  $iR$  drop between the reference and working electrodes is frequently very small. Thus, with the three-electrode system, the reference potential is much more stable, and there is compensation for the  $iR$  drop across the solution. This results in greater control over the working electrode potential. The counter electrode's function in the three-electrode configuration is to pass all of the current required to balance the current observed at the working electrode. To accomplish this task, the counter electrode frequently swings to extreme potentials.

#### **4. Conclusions and Future Perspective**

In this study, both paper electrode setups were successfully fabricated with the help of the screen-printing method, and we utilized these electrodes for the construction of a dengue aptasensor by employing silver/zinc nanocomposites. Both electrode setups were successfully capable in the determination of dengue virus, but the three-electrode system showed high current amplification as compared to the two-electrode system. Therefore, we can predict that in the

future, two-electrode systems will be completely replaced by the three-electrode system. This report gives the scientific community deeper insight into the electrode systems in terms of current amplification, fabrication methods, and their comparative features. In the future, such studies may be extremely beneficial to new researchers for obtaining good knowledge of the paper-based electrode setup, types of electrode setups, manufacturing technique of electrodes, different mechanisms of electrodes, and comparison of the two- and three-electrode systems. The present results show that the three-electrode arrangement is superior to the two-electrode setup. As a result, we will continue our research on the dengue aptasensor based on the three-electrode system only (and dropping the idea of the two-electrode system) by optimizing it on different parameters, trying to validate their results on human serum, and also modifying these three-electrode systems by using a paper-folding technique called origami, which may lead to the development of a novel report, i.e., origami-based dengue aptasensor.

## **5. Discussion**

No such reports are available on the comparison of paper electrode setups in terms of current enhancement. Two previous studies are compared in Table 4, which clearly reveals the current amplification using two- and three-electrode systems. The present work has shown a higher current amplification system as compared to previous studies.

**Table 4.** Comparison of existing reports with the present work.

Biosensor	Electrode System	Electrodes involved	Current Range (Approx.)	References
Electrochemical biosensor (zika virus)	Two-electrode system	Counter and working electrodes	2 $\mu$ A	[20]
Electrochemical biosensor (yellow fever)	Three-electrode system	Counter, working, and reference electrodes	180 $\mu$ A	[15]
Electrochemical biosensor (dengue virus)	Three-electrode system	Counter, working, reference electrodes	322.21 $\mu$ A	This work

## References

1. Santhiago, M.; Henry, C.S.; Kubota, L.T. Low cost simple three dimensional electrochemical paper-based analytical device for determination of p-nitrophenol. *Electrochim. Acta* **2017**, *130*, 771–777.
2. Anzar, N.; Hasan, R.; Tyagi, M.; Yadav, N.; Narang, J. Carbon nanotube—A review on Synthesis, Properties and plethora of applications in the field of biomedical science. *Sens. Int.* **2020**, *1*, 100003.
3. Kumanek, B.; Janas, D. Thermal conductivity of carbon nanotube networks: A review. *J. Mater. Sci.* **2019**, *54*, 7397–7427.
4. Hayat, A.; Marty, J.L. Disposable Screen-Printed Electrochemical Sensors: Tools for Environmental Monitoring. *Sensors* **2014**, *14*, 10432–10453.

5. Anzar, N.; Hasan, M.R.; Akram, M.; Yadav, N.; Narang, J. Systematic and validated techniques for the detection of ovarian cancer emphasizing the electro-analytical approach. *Process Biochem.* **2020**, *94*, 126–135.
6. Alam, A.; Hasan, M.R.; Anzar, N.; Suleman, S.; Narang, J. Diagnostic approaches for the rapid detection of Zika virus—A review. *Process Biochem.* **2020**, *101*, 156–168.
7. Ambaye, A.D.; Kefeni, K.K.; Mishra, S.B.; Nxumalo, E.N.; Ntsendwana, B. Recent developments in nanotechnology-based printing electrode systems for electrochemical sensors. *Talanta* **2020**, *225*, 121951.
8. Sengupt, A. Electrodes. *Metal Oxide Glass Nanocomposites*; Elsevier: Amsterdam, The Netherlands, 2020; pp. 249–257.
9. Singhal, C.; Dubey, A.; Mathur, A.; Pundir, C.; Narang, J. Paper based DNA biosensor for detection of chikungunya virus using gold shells coated magnetic nanocubes. *Process Biochem.* **2018**, *74*, 35–42.
10. Vasantham, S.; Alhans, R.; Singhal, C.; Nagabooshanam, S.; Nissar, S.; Basu, T.; Ray, S.C.; Wadhwa, S.; Narang, J.; Mathur, A. Paper based point of care immunosensor for the impedimetric detection of cardiac troponin I biomarker. *Biomed. Microdevices* **2019**, *22*, 6.
11. Mishra, A.; Pilloton, R.; Jain, S.; Roy, S.; Khanuja, M.; Mathur, A.; Narang, J. Paper-Based Electrodes Conjugated with Tungsten Disulfide Nanostructure and Aptamer for Impedimetric Detection of *Listeria monocytogenes*. *Biosensors* **2022**, *12*, 88.
12. Gupta, R.; Valappil, M.O.; Sakthivel, A.; Mathur, A.; Pundir, C.S.; Murugavel, K.; Narang, J.; Alwarappan, S. Tungsten disulfide Quantum Dots Based Disposable Paper Based Lab on GenoChip for Specific Meningitis DNA Detection. *J. Electrochem. Soc.* **2020**, *167*, 107501.
13. Glasscott, M.W.; Verber, M.D.; Hall, J.R.; Pendergast, A.D.; McKinney, C.J.; Dick, J.E. SweepStat: A build-it-yourself, two-electrode potentiostat for macroelectrode and ultramicroelectrode studies. *J. Chem. Educ.* **2020**, *97*, 265–270.

14. Teng, Y.; Chen, C.; Zhou, C.; Zhao, H.; Lan, M. Disposable amperometric biosensors based on xanthine oxidase immobilized in the Prussian blue modified screen-printed three-electrode system. *Sci. China Ser. B Chem.* **2010**, 53, 2581–2586.
15. Mehto, N.K.; Sharma, P.; Kumar, S.; Khanuja, M.; Rawal, R.; Narang, J. Towards papertronics based electrode decorated with zinc oxide nanoparticles for the detection of the yellow fever virus consensus sequence. *Process Biochem.* **2022**, 123, 36–43.
16. Narang, J.; Singhal, C.; Khanuja, M.; Mathur, A.; Jain, A.; Pundir, C.S. Hydrothermally synthesized zinc oxide nanorods incorporated on lab-on-paper device for electrochemical detection of recreational drug. *Artif. Cells Nanomed. Biotechnol.* **2018**, 46, 1586–1593.
17. Liu, J.; Morris, M.D.; Macazo, F.; Schoukroun-Barnes, L.R.; White, R.J. The Current and Future Role of Aptamers in Electroanalysis. *J. Electrochem. Soc.* **2014**, 161, H301–H313.

Mohd. Rahil Hasan (Phd, Scholar, applicant)



## 2. Experimental procedure (for Ovarian Cancer)

### 2.1. Materials required

binding aptamer [(5' -CCGATCTCTCCCACTCTCTCCA  
 ACTCACAGGCTACGGCACGTAGAGCATCACCATGATCCTGTGGG  
 TGTGTTGTTGATGGATCGGATCATCATGGTGAT-3' scale (uMole)]: 0.050)  
 16. PDGF from human platelets was purchased from MTOR LIFE SCIENCES PVT  
 LTD. PDGF was dissolved in PBS (Phosphate Bovine Serum) (pH-7.4, 100M). For  
 the preparation of synthetic serum: NaCl (Sodium chloride), CaCl<sub>2</sub> (Calcium



chloride), KCl (Potassium chloride), MgSO<sub>4</sub> (Magnesium sulphate), NaHCO<sub>3</sub> (Sodium bicarbonate), Na<sub>2</sub>HPO<sub>4</sub> (Disodium Phosphate), NaH<sub>2</sub>PO<sub>4</sub> (Monosodium Phosphate) were used. For the preparation of gold nanoparticles: Chloroauric acid (HAuCl<sub>4</sub>) (John Baker Inc.), trisodium citrate (LOBA), NaBH<sub>4</sub> (GRL Innovations), CTAB (HIMEDIA), Ascorbic acid (SRL) were used. All other chemicals are purchased from LOBA.

## **2.2. Apparatus**

Absorbance reading was taken using UV-VIS DOUBLE BEAM SPECTROPHOTOMETER (HALO DB-20R). The microstructural characterizations were performed by using X-ray diffraction (Smart Lab guidance, Rigaku) to check the phase and crystallinity. GNPs morphology were inspected via SEM on SEM ZEISS EVO18 at a voltage of 20 kV.

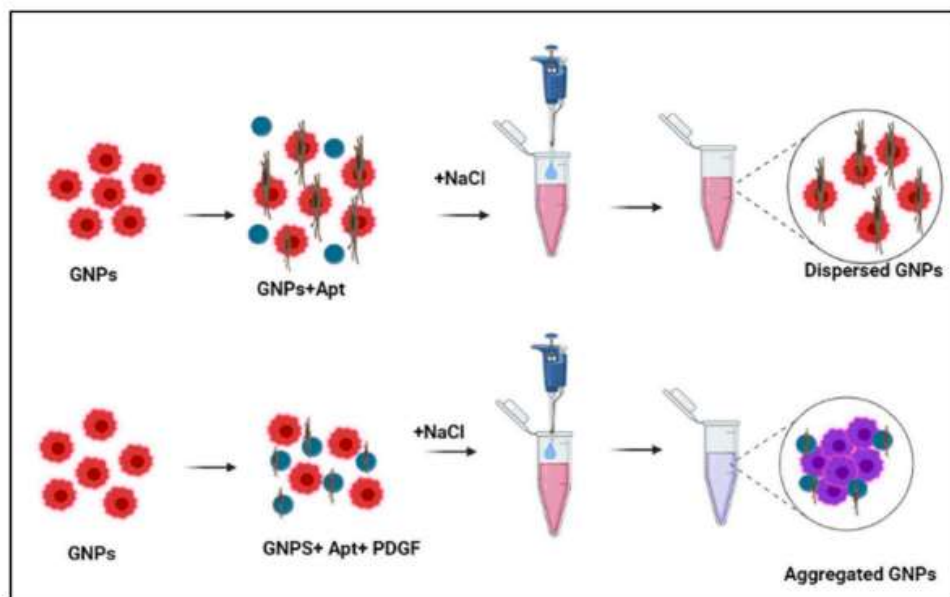
## **2.3. Preparation of gold nanoparticles**

CTAB and citrate-capped gold nanoparticles are prepared by seeded growth method reported by Jana et al. (2001). (a) Synthesis of seeds: HAuCl<sub>4</sub> (0.0005M) aqueous solution and trisodium citrate (0.0005M) aqueous solution were rapidly mixed for 10–15 min. Then freshly prepared 0.1M NaBH<sub>4</sub> (ice cold solution) were added slowly with stirring for 20 min then left undisturbed for 2–3 h; (b) Preparation of growth solution: CTAB powder was added in conical flask containing 200 ml of 0.0005 mM HAuCl<sub>4</sub> aqueous solution and mixture was heated to 50–60 °C until solution turned clear orange color; (c) Growth of seedling: Ascorbic acid (0.1M) aqueous solution was added in 36 ml of growth solution with stirring. After that 4 ml of seeds solution was added dropwise into the mixture with vigorous stirring for 10–20 min.

## **2.4. Procedure for naked eye sensing**

The procedure of naked eye sensing is very simple as it helps in colorimetric assay to detect PDGF by the help of naked eyes without using any instrument (Zhao et al., 2020). So, various concentration (0.01, 0.1, 1 and 10 µg/ml) of

platelet derived growth factors were added in plastic vials (2 ml) containing 26  $\mu\text{L}$  aptamer (10  $\mu\text{M}$ ). After incubation for 10 min, 596  $\mu\text{L}$  of the gold nanoparticles were added. Reacting for 5 min then 317  $\mu\text{L}$  of NaCl (0.25M) solution was transferred rapidly in-to the vials. Subsequently incubation for next 5 min, resulting solution was transferred into for UV-VIS spectroscopy.



**Scheme 1.** Schematic Representation of the GNPs-based colorimetric assay to diagnose PDGF. The scheme displays AuNPs, AptPDGF/Au NPs, and PDGF/AptPDGF/Au NPs.

### 3. Results & discussion

The morphology of gold nanoparticles was triangular in shape with an average edge length of 100 nm. SEM images revealed the presence of 2 geometries in the prepared sample including spheres and triangular nanoparticles, which are mainly dominated by truncated triangular nanoparticles (Aljabali et al., 2018).

UV-Vis spectroscopy is the most common method that used to measure attenuation of light, which reflects through the sample and give particular absorption peak at different wavelength, which confirms the successfully synthesis of the nanoparticles.

Fig. 1c) showing the absorbance of gold nanoparticles at 525 nm which confirmed the formation of nanoparticles. Fig. 1d) displays the X-ray diffraction pattern of GNPs. Four diffraction peaks are perceived that can be indexed to the (111), (2 00), (22 0), (311) & (222) reflections of face centered cubic structure of metallic gold, correspondingly represent that the manufactured GNPs are pure-crystalline gold composed (JCPDS No. 04-0784). The peak equivalent to (111) plane is more intense than the further planes signifying that (111) is the pre-dominant orientation.

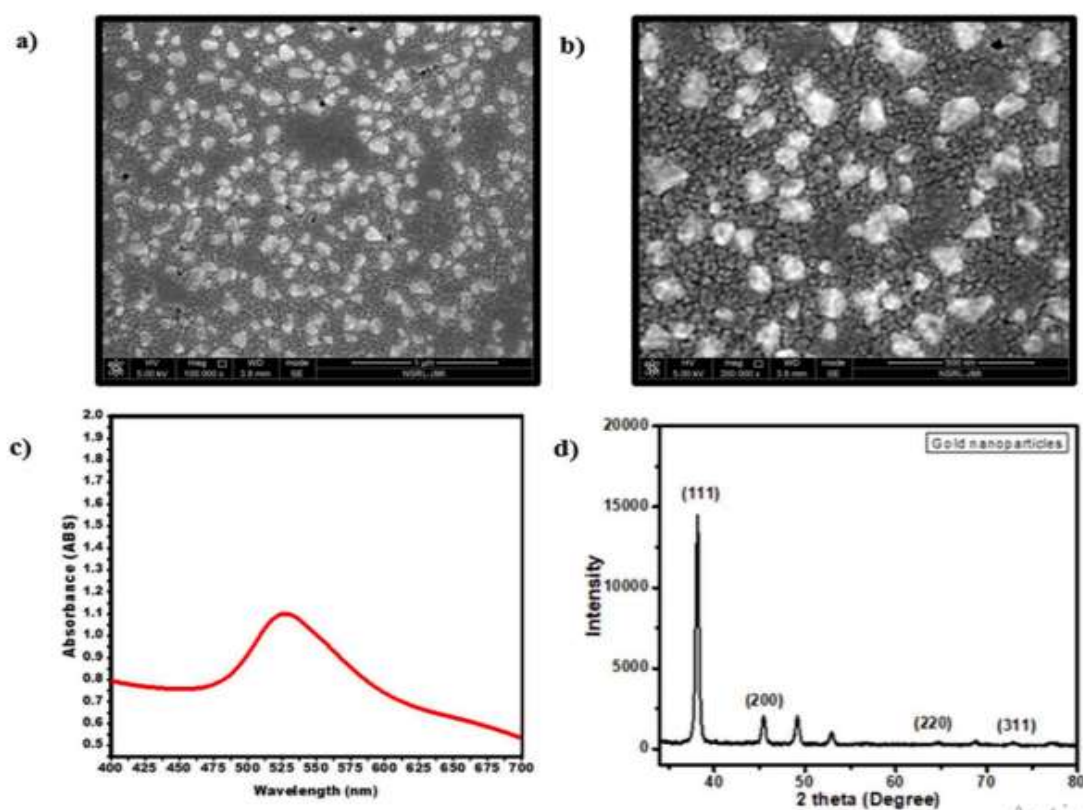


Fig. 1. a), b) GNPs-SEM images at the scale of 1 μm and 500 nm. c) UV-Vis spectroscopy of GNPs. d) XRD of GNPs.

### 3.1. Colorimetric diagnosis-principle

To established colorimetric assay for the detection of PDGF, firstly created citrate capped gold nanoparticles solution which helps to avoid the strong van der Waals attraction among GNPs which leads to the aggregation (Scheme 1). A random coil structure i.e., aptamer could bind to the particles of gold. These gold nanoparticles were remained dispersed despite of adding NaCl. Then target of

platelet derived growth factor is added which binds to the aptamer and induced the conformation to a rigid stem-loop structure. So that the aptamer lost the capability to defend the gold nanoparticles under salt concentration that leads to the GNPs-aggregation. Hence the GNPs-color changed (pinkish-light purple). The aptamer & GNPs changed color in the existence of platelets derived growth factors. These PDGF was used in different concentration which depict the different color variation. While using PDGF in very lower concentration, than there is no clear aggregation was observed and again, there is no clear aggregation while using the high concentration of platelets derived growth factor.

### **3.2. Colorimetric assay-Optimization**

Optimization is one of the leading steps for any research, as it helps to adjust the performance of the proposed system, Similarly, in this work optimization is done for the colorimetric biosensor to detect PDGF, various PDGF-concentration was optimized than urea sample is used to check the specificity and effect of salt along with stability is also optimized. At the last analysis is done by using real sample to investigate this experiment.

#### **3.2.1. Different concentration of PDGF**

The concentration of platelet derived growth factor i.e., from 0.01 to 10  $\mu\text{g/ml}$  increases with the increase in the absorbance at the wavelength of 525 nm (Fig. 2a). The experiment was conducted for five times for each concentration and it was seen that the results was approximately same at every repeated cycle. It was inferred from experimental results that the assay was reproducible as seen in Fig. 2b. Furthermore, Fig. 2c represents naked eye observation of PDGF when introduced with aptamer and AuNPs. As the concentration of PDGF increases the color of assay change from pink to light purple as it gets aggregated. The urea has been taken as the interferant, and there was no color change or aggregation and remained pink in color and almost same as the color of aptamer.

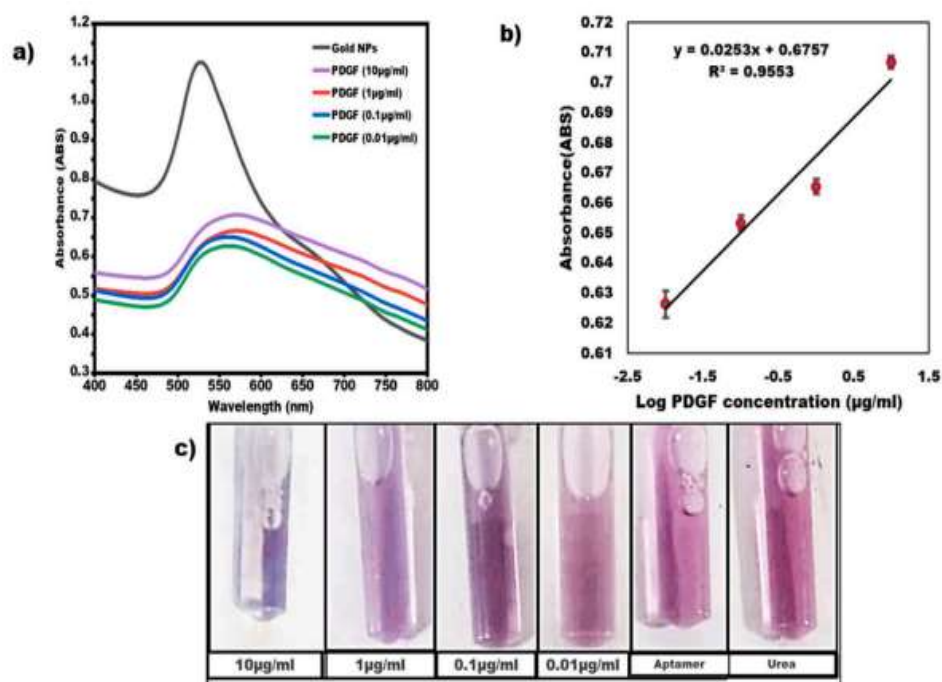


**Fig. 2.** Different concentration of Au NPs based colorimetric method. (a) UV-spectrophotometer shows the absorption of Au NPs alone & and PDGF/AptPDGF/Au NPs (10 µg/ml, 1 µg/ml, 0.1 µg/ml and 0.01 µg/ml). aptamer introduced in the presence of PDGF. (b) Error bar represents the standard deviation of the assay for each concentration repeated for 5 times. (c) Naked eye observation of PDGF at various concentrations introduced with aptamer & GNPs. Various concentration of platelet derived growth factors were added in plastic vials (2 ml) containing 26 µL aptamer (10 µM). After incubation for 10 min, 596 µL of the gold nanoparticles were added. Reacting for 5 min then 317 µL of NaCl (0.25M) solution was transferred rapidly in-to the vials. Subsequently incubation for next 5 min, resulting solution was transferred into for UV-VIS spectroscopy. (For interpretation of the references to color in this figure legend, the reader is referred to the Web version of this article.)

### 3.2.2. Specificity and reliability

This colorimetric assay selectivity was estimated through analysis with urea. Reactivity was observed only in PDGF. Result displays that there was no major change in the UV-Vis absorbance peak of gold nanoparticles before & after the addition of urea respectively, the pink color remained unchanged (Fig. 3a). This study concluded that the urea had no specific binding to the aptamer of PDGF, therefore, no aggregation occurred. But, in presence of PDGF, gold nanoparticles aggregates & the absorbance at 525 nm decreased. For validation of the above results, Fig. 3b, bar graph has been represented.

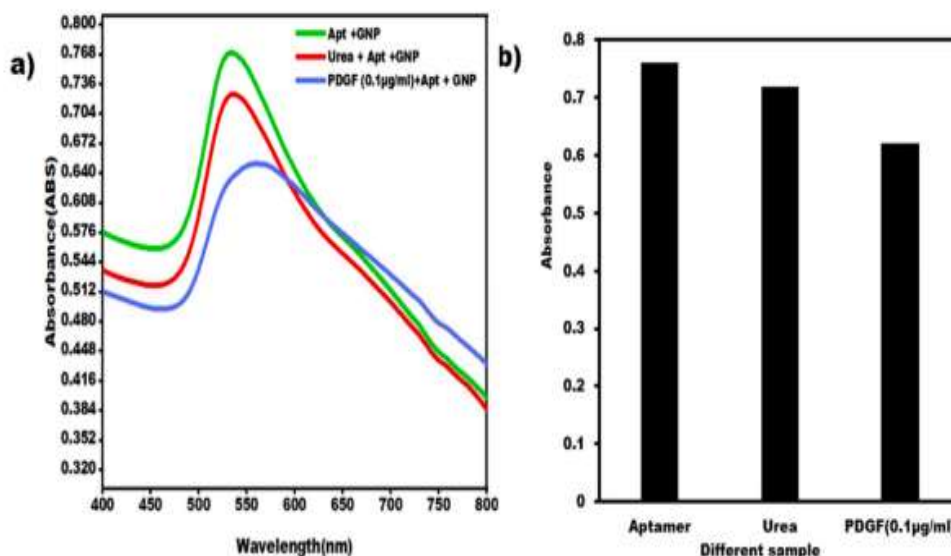


Fig. 3. UV-vis absorption spectra of solutions of AptPDGF/Au NPs, Urea/AptPDGF/Au NPs and PDGF/AptPDGF/Au NPs. B) Bar graph representing absorption value of AptPDGF/Au NPs, Urea/AptPDGF/Au NPs and PDGF/AptPDGF/Au NPs. All experimental conditions are same as described in Fig. 2.

### 3.2.3. Analysis on real sample (synthetic serum)

Au NPs -based colorimetric assay was evaluated for its proficiency and feasibility to diagnose PDGF in real sample. In this experiment, PDGF (10 µg) was dissolved in synthetic serum.

In Fig. 4, the test is capable to diagnose PDGF from synthetic serum samples within few minutes. Results were also compared with the control i.e., distilled water. Overall, the outcomes of this experiment confirmed that this gold nanoparticles based colorimetric assay to detect PDGF could be appropriate alternative used for predictable study of PDGF in real samples.



**Fig. 4.** Validation of the AptPDGF/Au NPs probe for the detection of PDGF in Synthetic serum cell spiked with PDGF (10 µg/ml).

#### **4. Conclusion**

This proposed research, demonstrated a colorimetric biosensor to diagnose platelets derived growth factor by using AuNPs. There are numerous advantages of using this assay such as simple, sensitive and low cost. Platelets derived growth factor is sensitively & specifically diagnosed by the help of AuNPs & Aptamer with the linear range: 0.01–10 µg/ml and limit of detections found to be 0.01 µg/ml. Besides, the variation of different concentration could be assessed with naked eyes. Thus, the given platform is a simple approach that does not require costly apparatus and can be used to diagnose ovarian cancer with good sensitivity and specificity. This technology might potentially be used as a universal means of ovarian cancer screening testing, allowing patients to obtain early and actual treatment. This proposed theory concludes that the detection of PDGF might be possible with naked eye. Future efforts might be directed towards building aptamer-based probes that employ other types of nanomaterials and different morphology of NPs, such as gold nanorods (Au NRs), to improve sensitivity. To further increase the dynamic range of these aptamer

nanoparticle-based probes, it will be necessary to decrease nonspecific adsorption of proteins and DNA by altering the surfaces to improvise the sensing platform. The developed approach can be linked with electronic readout for more easy and simplistic detection.

## References

- Aljabali, Alaa A.A., et al., 2018. Synthesis of gold nanoparticles using leaf extract of *Ziziphus zizyphus* and their antimicrobial activity. *Nanomaterials* 8 (3), 174.
- Anzar, N., Hasan, M.R., Akram, M., Yadav, N., Narang, J., 2020. *Process Biochem.* 94, 126–135.
- Apte, Sachin M., Corazon, D., Bucana, Jerald J., Killion, David M., Gershenson, and Isaiah J., Fidler, 2004. *Gynecologic Oncology* .vol. 1,78-86.
- De, La, Franier, B., 2019. *Biosens. Bioelectron.* 135, 71–81. Henriksen, R., Funa, K., Wilander, E., Backstrom, T., Ridderheim, M., Oberg, K., 1993. *Cancer Res.* 53 (19), 4550–4554.
- Huang, C.C., Huang, Y.F., Cao, Z., Tan, W., Chang, H.T., 2005b. *Anal. Chem.* 77 (17), 5735–5741.
- Jana, N.R., Gearheart, L., Murphy, C.J., 2001. *Langmuir* 17 (22), 6782–6786.
- Jazayeri, M.H., Aghaie, T., Avan, A., Vatankhah, A., Ghaffari, M.R., 2018. *Sens. Bio-sens. Res.* 20, 1–8.
- La, Rochelle WJ., Jeffers, M., Mc, Donald, Wf, Chillakuru RA., Giese, N.A., Lokker, N.A., Sullivan, C., Boldog, F.L., Yang, M., Vernet, C., Burgess, C.E., 2001. *Nat. Cell Biol.* 3 (5), 517–521.
- Lin, T.E., Chen, W.H., Shiang, Y.C., Huang, C.C., Chang, H.T., 2011. *Biosens. Bioelectron.* 29 (1), 204–209.



Morais, M.G., Martins, V.G., Steffens, D., Pranke, P., da Costa, J.A., 2014. J. Nanosci. Nanotechnol. 14 (1), 1007–1017.

Nejati, K., Dadashpour, M., Gharibi, T., Mellatyar, H., Akbarzadeh, A., 2021. J. Cluster Sci. 3, 1–6.

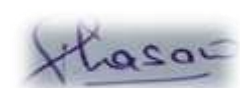
Reid, BM., Permuth, JB., Sellers, TA., Cancer Biol. Med..1,9. Severino, P., De, Hollanda, Lm, Santini, A, Reis, Lv, Souto, Sb, Souto, Eb, Silva AM., 2016. William Andrew Publishing pp, 91-115.

Sharma, P., Panchal, A., Yadav, N., Narang, J., 2020. Int. J. Biol. Macromol. 155, 685–696.

Versnel, M.A., Haarbrink, M., Langerak, A.W., de, Laat PA., Hagemeijer, A., van der, Kwast TH., et al., 1994. Cancer Genet. Cytogenet. 73 (1), 60–64.

Zhao, V.X., Wong, T.I., Zheng, X.T., Tan, Y.N., Zhou, X., 2020. Mater. Sci. Energy Technol. 3, 237–249.

**Mohd. Rahil Hasan (Phd, Scholar, applicant)**

A handwritten signature in blue ink, appearing to read 'H. Hasan', is shown on a light blue background.